INTRODUCTION

Although the pathogenesis of rheumatoid arthritis (RA) remains as yet unclear, it has long been suggested that activation of the innate immune system by endogenous or exogenous stimuli contribute to its pathogenesis (1, 2). Fungal, bacterial and viral pathogens but also endogenous danger signals e.g. heat-shock proteins are recognized by specific pattern-recognition receptors, such as Toll-like receptors (TLRs) and nucleotide-binding oligomerization domain (NOD)-like receptor (NLRs). While TLRs are cell-surface or endosomal receptors, NLRs are cytosolic molecules. Both TLRs and NLRs mediate the production of proinflammatory mediators via initiation of the transcription factor NF-κB and the MAP kinase cascade (3, 4).

Recently, we have demonstrated that RA synovial fibroblasts (RASFs) express specific TLRs and the NLR NOD2, and that their activation plays a role in the pathogenesis of RA by induction of proinflammatory cytokines, chemokines, and matrix degrading enzymes (5-7). Together with NOD2, NOD1 belongs to the group of caspase-activation and recruitment domain (CARD) containing NLRs and is known to be expressed in antigen-presenting cells and epithelial cells (8, 9). It senses the peptidoglycan-related molecule diaminopimelic acid (DAP) which is a constituent of most Gram-negative bacteria and specific Gram-positive bacteria such as *Listeria* and *Bacillus spp* (10). NOD1 has been found to be crucial for host defence against a variety of bacteria including *Helicobacter pylori* and *Chlamydiae* (11, 12). Accordingly, it was shown to induce an inflammatory response in many different cell types and to synergize with TLR receptors to coordinate the immune defense (9, 13, 14). Moreover, a polymorphism in NOD1 was shown to be associated with susceptibility to chronic inflammatory diseases such as asthma and inflammatory bowel disease (15, 16).

To clarify the role of NOD1 in RA and its possible interaction with other innate immune pathways, we analyzed the expression of NOD1 in synovial tissues and synovial fibroblasts (SFs). We show expression, regulation, and function of NOD1 in synovial cells and found a

novel role of NOD1 in promoting TLR2 signaling pathways in synovial fibroblasts.

MATERIALS AND METHODS

Synovial tissues and culture of synovial fibroblasts, peripheral blood mononucleated cells (PBMCs) and monocyte-derived macrophages (MDM)

RA and osteoarthritis (OA) synovial tissues were obtained from patients undergoing joint replacement surgery (Schulthess Clinic, Zurich, Switzerland). Gout or psoriasis arthritis (PA) synovial tissues were obtained from biopsies. All patients signed a consent form before procedure and the study was permitted by the local ethical authorities. Patients with RA fulfilled the revised criteria from the American College of Rheumatology (ACR) for classification of RA (17). SFs were isolated by digestion of the synovial tissues (150 mg/ml dispase, 37°C, 60 minutes) and cultured in Dulbecco's minimum essential medium (Gibco Invitrogen, Basel, Switzerland) supplemented with 10% foetal calf serum (FCS), 50 U/ml penicillin/streptomycin, 2 mM L-glutamine, 10 mM HEPES, and 0.2% amphotericin B (all from Gibco Invitrogen). Cell cultures were maintained at 37°C in a humidified 5% CO_2 incubator. For the experiments, cultured SFs from passages 4 to 8 were used.

PBMCs were isolated from EDTA-blood of healthy donors using Ficoll-Paque PLUS gradient centrifugation. For the generation of MDMs, peripheral blood monocytes were isolated from PBMCs with CD14 MACS MicroBeads (Miltenyi Biotec, Bergisch Gladbach, Germany) and 15 ng/ml macrophage-colony stimulating factor (HumanZyme, Chicago, IL) was added every 48 hours for 7 days. MDMs and PBMCs were cultured in RPMI1640 (Gibco Invitrogen) supplemented with 10% FCS, 50 IU/ml penicillin-streptomycin, 2 mM L-glutamine, 10 mM HEPES, and 0.2% fungicide.

Immunohistochemistry/Immunofluorescence

For immunohistochemistry, sections from formalin-fixed, paraffin-embedded tissues were deparaffinised and pretreated at 80°C for 30 minutes in 10 mM citrate buffer (pH 6.0) for

antigen retrieval. After washing in H_2O, sections were incubated with 3% H_2O_2. Washing in phosphate buffered saline (PBS)/0.05% Tween was followed by 1 hour incubation in PBS/0.05% Tween/5% goat serum/1% bovine serum albumin (= blocking buffer). The sections were incubated overnight at 4°C with rabbit anti-human NOD1 antiserum (2 µg/ml; Alpha Diagnostic, San Antonio, TX). As negative control, rabbit IgG was used instead of the primary antibody. To show specificity of NOD1 antibody binding, additional antibody-blocking experiments were performed. Thereby 1 µg antibody was incubated with or without 50 µg blocking peptide (Alpha Diagnostic) at 37°C for 2 hours and then at 4 °C for 24 hours. The solutions were centrifuged for 15 minutes at 14000 rpm. Supernatants were then used as primary antibodies. After washing, all slides were incubated for 30 minutes with horseradish peroxidase (HRP)-conjugated goat anti-rabbit IgG (Jackson ImmunoResearch, Soham, UK). Antigen-antibody complexes were detected with aminoethylcarbazole chromogen substrate (DakoCytomation, Glostrup, Denmark) and counterstained with hematoxylin. The intensity of the staining was evaluated in the lining and the sublining by two observers following a gradual scale ranging from 0 (no staining) to 4 (strong staining).

For immunofluorescence double stainings, deparaffinised slides were pre-treated with 10 mM citrate buffer as described above, followed by incubation in 1 mg/ml trypsin (Sigma-Aldrich, Buchs, Switzerland) at 37°C for 20 minutes. Unspecific protein binding was blocked with blocking buffer for 1h. Slides were incubated with rabbit anti-human NOD1 antiserum plus mouse anti-human CD68 (clone PG-MA; DakoCytomation) or plus mouse anti-human vimentin (DakoCytomation) at 4°C for 24 hours (all at 2 µg/ml). 2 µg/ml rabbit IgG and mouse IgG served as negative control. Goat anti-rabbit Texas Red labeled antibodies and goat anti-mouse AlexaFluor488 labeled antibodies (both Jackson ImmunoResearch) were used as secondary antibodies. Nuclei were stained with DAPI.

Stimulation experiments

Cells were stimulated with the following agents: 10 ng/ml L-alanyl-γ-D-glutamyl-meso-

diaminopimelic acid (Tri-DAP) (InvivoGen, San Diego, CA), 10 μg/ml polyI:C (PIC) (InvivoGen), 100 ng/ml lipopolysaccharide (LPS) from *Esherichia coli* (List Biological Laboratories, Campbell, CA), 300 ng/ml palmitoyl-3-cystein-serine-lysine-4 (Pam3) (InvivoGen), 1 ng/ml interleukin-1β (IL-1β) (R&D Systems, Minneapolis, MN), 10 ng/ml tumor necrosis factor-α (TNF-α) (R&D Systems), 10^9 cells/ml heat-inactivated *Staphylococcus aureus* or heat-inactivated *Listeria monocytogenes* (InvivoGen) or 5 ng/ml polymyxin B (Sigma-Aldrich).

Quantitative Real-time polymerase chain reaction

Total RNA was isolated with the RNeasy Mini Kit (Qiagen, Basel, Switzerland) and cDNA was generated by reverse transcription using random hexamers and multiscribe reverse transcriptase (Applied Biosystems, Rotkreuz, Switzerland). Expression levels of mRNAs were determined by Taqman/SYBR Green real-time PCR on an ABI PRISM 7500 Sequence Detection System (Applied Biosystems). The sequence of primers and probes used for the detection of MMPs and TLRs are published in (7) and (6), the sequences for the SYBR primers used are as follows: **NOD1**: FORWARD gag caa agt cgt ggt caa ca; REVERSE gct gct ggg tat acc tgc tc; **NOD2:** FORWARD ttc tcc ggg ttg tga aat gt; REVERSE ctc ctc tgt gcc tga aaa gc; **IL-6:** FORWARD ctc ttc aga acg aat tga caa aca a; REVERSE gag atg ccg tcg acg atg tac; **CCL5:** FORWARD ctc ccc ata ttc ctc gga ca; REVERSE gcg ggc aat gta ggc aaa.

The expression of the housekeeping gene 18S was used as endogenous control. For calculations of fold changes, the comparative threshold cycle (Ct) method was used as previously described (6).

Silencing of NOD1

RASFs were transfected using Amaxa Basic Nucleofector kit (Lonza, Basel, Switzerland) according to the manufacturer's protocol. Briefly, cells (5 x 10^5) were resuspended in 100 μl of transfection solution, with 2.0 μg of control siRNA/NOD1 siRNA (Ambion, Austin, TX) and transfection was done using a nucleofector device (Program U23). After 24 hours of

transfection, medium was changed and cells stimulated. Silencing of NOD2 was done as previously described (18).

ELISAs

The detection of IL-6 protein in cell supernatants was performed with an OptEIA kit (BD PharMingen, San Diego, CA) according to the manufacturer's instructions. For measurements of CCL5, MMP-1 and MMP-3 DuoSet ELISA Development kits were used (R&D Systems, Minneapolis, MN).

Flow cytometry

Cells were detached with accutase (PAA laboratories, Pasching, Austria) and washed with 1% FCS in PBS. 2 µl mouse anti-human TLR2 antibodies (eBioscience, San Diego, CA) or mouse IgG2a kappa were added to 1 x 10^5 cells and incubated for 30 minutes at 4°C. After washing, cells were treated with 1 µl FITC labelled goat anti-mouse IgGs (Jackson ImmunoResearch) for 30 minutes at 4°C. Cells were washed and resuspended in 1% FCS in PBS and analyzed on a FACSCalibur flow cytometer. Data were processed using CellQuest software (BD Biosciences, Dan Diego, CA)

NOD1 protein was detected by intracellular staining using the BD Cytofix/Cytoperm kit (BD PharMingen). Permeabilized cells were incubated for 30 minutes at 4°C with 1 µg/ml of rabbit anti-human NOD1 antiserum (Alpha Diagnostic) or goat anti rabbit IgG as isotype control. Cells were washed with BD Perm/Wash solution and subsequently incubated for 30 minutes at 4°C with 0.5 µg/ml of FITC-labeled goat anti-rabbit Ig (BD PharMingen). After 2 more washing steps with BD Perm/Wash solution, cells were resuspended in 1% FCS in PBS and analyzed on a FACSCalibur flow cytometer. Data were processed using CellQuest software (BD Biosciences). To show specificity of the binding of NOD1 antibodies, antibody-blocking experiments were performed as described for immunohistochemistry. The blocking peptide blocked > 90% of NOD1 staining.

Western blotting

Whole cell lysates were dissolved in sample buffer (50mM Tris-HCl buffer pH6.8, 0.4% SDS, 10% glycerol, 1.5% β-mercaptoethanol and 0.001% bromophenol blue) and boiled at 95 °C for 3 minutes. Proteins were separated in a SDS polyacrylamide gel and transferred to nitrocellulose membranes. Membranes were blocked with 5% nonfat dry milk for 1 h at room temperature, and then incubated overnight at 4°C with rabbit anti-human phospho (Thr 209) – IRAK1 (Abcam, Cambridge, UK), mouse anti-human NOD2 (clone 2D, Santa Cruz Biotechnology, Santa Cruz, CA), mouse anti-human tubulin (SigmaAldrich), or mouse anti-human β-actin (Sigma-Aldrich) antibodies. The membranes were washed and then incubated for 45 minutes with the respective HRP-conjugated secondary antibodies. After washing, antigen-antibody complexes were detected with ECL Western Blotting kit (GE Healthcare, Buckinghamshire, UK). Protein levels were analyzed by Calibrated Densitometer (BIO-RAD, Hercules, CA).

Statistical analysis

Values are presented as the mean ± SEM. Mann-Whitney U test or Wilcoxon Singed Rank Test (paired samples) were applied to compare 2 groups. Non-parametric Friedman test followed by Dunn's multiple comparison test was used for multiple comparisons and synergistic interaction was calculated by TwoWay ANOVA with Replication. P values less than 0.05 were considered statistically significant.

RESULTS

Expression of NOD1 protein in RA and OA synovial tissues

We analyzed the expression of NOD1 in synovial tissues of patients with RA (n=9) and OA (n=6) by immunohistochemistry and found NOD1 to be strongly expressed in RA patients (Fig.1A). Scoring of NOD1 protein expression showed that in RA synovial tissues expression of NOD1 protein was significantly increased in the lining and sublining areas compared to OA synovial tissues. The addition of a synthetic NOD1-blocking peptide blocked staining by

NOD1 antibodies, proving the specificity of the staining (inset Fig. 1A).

To see which cells in the synovium express NOD1 we did double stainings for NOD1 and either the macrophage marker CD68 or vimentin as a mesenchymal cell marker. Macrophages as well as synovial fibroblasts and endothelial cells stained positive for NOD1 (Figs.1B and C).

NOD1 expression was also tested in patients with gout (n=6) and psoriasis arthritis (PA; n=4). While only one out of four PA synovial tissues expressed NOD1, all of the gout synovial tissues displayed strong staining for NOD1 (Fig.1D).

Expression and regulation of NOD1 in different cell types

We next examined expression and regulation of NOD1 in RASFs, OASFs, healthy PBMCs and MDMs. NOD1 was expressed by all the tested cells and there was no significant difference in the basal expression of NOD1 mRNA or protein in the different cell types (Fig. 2A). Stimulation experiments showed that levels of NOD1 were significantly up-regulated by the TLR3 ligand PIC in RASFs, while the NOD1 ligand Tri-DAP, the TLR2 ligand Pam3, the TLR4 ligand LPS, TNF-α or IL-1β had no effect on NOD1 transcription (Fig. 2B). In contrast, in MDMs neither NOD1 mRNA nor protein levels were changed by stimulation with any of the tested TLR ligands (Fig. 2C).

Expression of proinflammatory and matrix degrading molecules after stimulation with the NOD1 ligand

To learn more about the function of NOD1 signaling in synovial fibroblasts, we stimulated RASFs with the NOD1 ligand Tri-DAP and measured mRNA expression of the proinflammatory cytokine IL-6, the chemokine CCL5 (RANTES), matrix metalloproteinases and the PRRs TLR2, TLR3, TLR4 and NOD2. Expression of IL-6 and CCL5 mRNA was significantly up-regulated after 8h and 24h stimulation with Tri-DAP (Fig. 3A). Whereas the mean increase of IL-6 was 4 fold, levels of CCL5 were induced more than 20 fold by NOD1 activation. Also the expression of MMP-1, MMP-3, and MMP-13 mRNA was significantly

up-regulated by Tri-DAP (Fig. 3B). With a 6 fold increase MMP-1 mRNA was induced the strongest, followed by MMP-3 which was induced 5 fold and MMP-13 with a 4 fold increase after 8h. MMP-9 mRNA was increased in some RASFs after stimulation but the change did not reach statistical significance. Regarding PRRs, TLR3 and TLR4 expression was not induced by the NOD1 ligand, whereas TLR2 was 6 fold up-regulated by Tri-DAP after 8h stimulation (Fig. 3C). Also NOD2 expression was induced by NOD1 signalling, however a significant change was only seen after 24h stimulation (Fig. 3D). Increased expression of IL-6 (Fig. 4A), CCL5, MMP-1, MMP-3, TLR-2 and NOD2 after stimulation of RASFs with Tri-DAP were also confirmed on protein level (supplemental Fig. 1).

Additional time course experiments showed that stimulation of NOD1 in RASFs induced pro-inflammatory mediators and MMPs in a rapid response reaction (4h) and only at a later time point the expression of TLR2 (8h) and NOD2 (24h) were upregulated (Supplemental Fig. 2). We also looked whether stimulation with Tri-DAP can induce TLR ligands in MDMs, but no change in the expression of TLR2, TLR3 and TLR4 was seen after 24h stimulation with Tri-DAP (n=3, data not shown).

To ensure that the pro-inflammatory response seen after stimulation with Tri-DAP was not due to endotoxin contaminations we added polymyxin B which can neutralize the effect of LPS. No difference between Tri-DAP and Tri-DAP plus polymyxin B stimulated cells in the induction of IL-6 was seen, confirming an endotoxin-free preparation of the used Tri-DAP (Fig. 4A). For further confirmation that the measured effects after stimulation with Tri-DAP were solely mediated by the NOD1 receptor, we silenced expression of NOD1 with siRNA (Fig. 4B). Knock-down of the receptor indeed abolished the stimulatory effect of Tri-DAP in RASFs (Fig. 4C).

NOD1 synergizes with TLR2 and TLR4 in RASFs and promotes TLR2 and IL-1 signaling

Previously it was reported that NOD1 can synergize with TLR2 and TLR4 in the production

of IL-6 and IL-1β in human monocytes, dendritic cells and PBMCs (9, 14). To elucidate a possible crosstalk between NOD1 and TLR pathways in RASFs co-stimulation experiments with Tri-DAP and the TLR2 ligand Pam3, the TLR3 ligand PIC and the TLR4 ligand LPS were done. Similar to published results in immune cells also in RASFs, a synergistic effect of simultaneous stimulation of NOD1 with TLR2 and TLR4, but not with TLR3 was found (Fig. 5A).

Since a modulating effect of NOD1 on TLR2/NOD2 signalling pathways has been suggested in mice (19), we tested whether knock-down of NOD1 would have any influence on IL-6 production after TLR stimulation. While the absence of NOD1 did not alter the response to TLR3 or TLR4 activation, IL-6 levels were 24% lower after TLR2 stimulation when NOD1 was knocked-down, suggesting a promoting role for NOD1 in TLR2 signaling (Fig 5B). No such effect was seen when NOD2 was knocked-down, where levels of IL-6 were the same after TLR2 stimulation in control transfected cells and siNOD2 transfected cells (Fig. 5B).

We then tested whether the modulating effect of NOD1 would still be effective, if TLR2 pathways were not selectively activated, but in combination with other pattern recognition receptors. The cell wall of *Staphylococcus aureus* contains TLR2 activating peptidoglycans as well as NOD2 activating muramyl dipeptides (MDP). The cell wall of *Listeria monocytogenes* in addition contains DAP and therefore stimulates TLR2, NOD2 and NOD1 pathways. The double and triple activation of PRRs overruled the modulating effect of NOD1 seen with specific TLR2 stimulation alone and no difference in IL-6 production between NOD1 silenced and control RASFs was seen (Fig. 5C left panel). Since this specific effect of NOD1 silencing on TLR2 signaling could be due to downregulation of TLR2 itself by NOD1 silencing, we measured TLR2 transcripts after silencing of NOD1. As described before TLR2 levels were strongly increased after incubation of RASFs with TLR2 ligands, but silencing of NOD1 had no effect on TLR2 levels in unstimulated or stimulated cells (Fig. 5C right panel).

From the three TLRs analyzed TLR2 is the only one that exclusively signals via the adaptor

protein MyD88. Therefore, we hypothesized that NOD1 might influence the MyD88 signaling pathway. If this was the case, then NOD1 knock-down should diminish IL-1 signaling, since MydD88 is also recruited by the IL-1 receptor after ligand binding. Stimulation of NOD1 knocked-down cells with IL-1β led to 18% less production of IL-6 than IL-1β stimulation in control transfected cells, corroborating a modulating role of NOD1 in the MyD88 pathway (Fig. 5D).

Activation of MyD88 leads to phosphorylation of the interleukin-1 receptor-associated kinase IRAK1. Accordingly we found that stimulation of RASFs with Pam3 increased phosphorylation of IRAK1 20 min after stimulation (Fig. 6). Knock-down of NOD1 however prevented IRAK1 phosphorylation after Pam3 stimulation.

DISCUSSION

In the current study, we show that NOD1 is strongly expressed in RA synovium and that its expression can be induced in RASFs by stimulation of TLR3. NOD1 stimulation of RASFs led to a rapid increase in the production of pro-inflammatory and matrix-degrading mediators, followed by up-regulation of the expression of TLR2 and NOD2 and synergized with TLR2 and TLR4 stimulation in the production of IL-6. Finally, knock-down of NOD1 diminished IL-6 production after stimulation with Pam3 and IL-1β and blocked phosphorylation of IRAK1.

As shown in our results NOD1 expression is equally high in synovial fibroblasts, macrophages and PBMCs. Furthermore, TLR3 stimulation further increased expression of NOD1 in RASFs. The high levels of NOD1 in RA synovial tissues compared to OA synovial tissues is therefore most probably based on influx of immune cells in the synovium on the one hand, and higher NOD1 expression in RASFs caused by TLR3 activation on the other. It has been shown that endogenous double-stranded RNA from necrotic cells can activate RASFs via TLR3, which might be the mechanism by which expression of NOD1 is increased in

RASFs in vivo (5). The high expression of NOD1 which we found in gout points to a pathophysiological role of NOD1 also in this disease. Similar to the NOD-like receptor protein 3 (NLRP3) inflammasome, which is well known to play an important role in gout, NOD1 has been shown to bind to caspase 1 and promote IL-1 secretion (20).

Stimulation of NOD1 led to the production of a wide range of pro-inflammatory mediators and MMPs in RASFs. In addition there was a synergistic effect in the production of IL-6 by stimulation of NOD1 and TLRs. Surprisingly, MDMs reacted much less to stimulation with Tri-DAP than synovial fibroblasts. Together these data underline the important role of synovial fibroblasts as cells of the innate immune system that rapidly integrate and elicit an innate immune response. Of special interest seems the fact that stimulation of NOD1 selectively induced increased expression of other peptidoglycan sensing PRRs, namely TLR2 and NOD2, but not TLR4 and TLR3. This points to a directed chain reaction for proper immune defense rather than to a general increase in PRRs after sensing of invading pathogens. Exogenous ligands for PRRs such as the NOD2 ligand MDP or bacterial peptidoglycans were described to be present in joints of RA patients (19, 21). Also more and more endogenous ligands for PRRs are found and it has become clear that in addition to their role in immune defence, PRRs are also important sensors of tissue damage. No endogenous ligands for the NLRs NOD1 and NOD2 have been found up to now. In fact, it has to be mentioned that also direct interactions of NOD1 and NOD2 with their respective ligands were not demonstrated yet. Thereby indirect mechanisms by which these NLRs respond to their ligands cannot be excluded. The current study suggests that the presence of NOD1 is essential for the phosphorylation of IRAK1 after recruitment to MyD88. This is particularly interesting since NLRP12, a member of the pyrin-domain containing NLR subfamily, has been shown to bind IRAK1 and to block its phosphorylation (22). In general, evidence accumulates that NLRs tend to associate with other proteins to form large complexes and that the composition of this complexes determines the biological function of the various NLRs (23).

In summary, we show increased expression of NOD1 in synovial tissues of RA patients and a strong pro-inflammatory response of RASFs after stimulation of NOD1 with its ligand Tri-DAP. Downregulation of NOD1 led to reduced levels of IL-6 after TLR2 as well as IL-1β stimulation and blocked phosphorylation of IRAK1. Therefore, our data indicate that NOD1 alone and in interaction with other inflammatory activators plays an important role in the chronic and destructive joint inflammation in RA.

Acknowledgements: We thank Peter Künzler, Ferenc Pataky and Maria Comazzi for invaluable technical advice and assistance.

REFERENCES

1. Zhang X, Glogauer M, Zhu F, Kim TH, Chiu B, Inman RD. Innate immunity and arthritis: neutrophil Rac and toll-like receptor 4 expression define outcomes in infection-triggered arthritis. Arthritis Rheum. 2005;52(4):1297-304.
2. Deng GM, Nilsson IM, Verdrengh M, Collins LV, Tarkowski A. Intra-articularly localized bacterial DNA containing CpG motifs induces arthritis. Nat Med. 1999;5(6):702-5.
3. Strober W, Murray PJ, Kitani A, Watanabe T. Signalling pathways and molecular interactions of NOD1 and NOD2. Nat Rev Immunol. 2006;6(1):9-20.
4. Franchi L, Warner N, Viani K, Nunez G. Function of Nod-like receptors in microbial recognition and host defense. Immunol Rev. 2009;227(1):106-28.
5. Brentano F, Schorr O, Gay RE, Gay S, Kyburz D. RNA released from necrotic synovial fluid cells activates rheumatoid arthritis synovial fibroblasts via Toll-like receptor 3. Arthritis Rheum. 2005;52(9):2656-65.
6. Ospelt C, Brentano F, Rengel Y, Stanczyk J, Kolling C, Tak PP, et al. Overexpression of toll-like receptors 3 and 4 in synovial tissue from patients with early rheumatoid arthritis: toll-like receptor expression in early and longstanding arthritis. Arthritis Rheum. 2008;58(12):3684-92.
7. Ospelt C, Brentano F, Jungel A, Rengel Y, Kolling C, Michel BA, et al. Expression, regulation, and signaling of the pattern-recognition receptor nucleotide-binding oligomerization domain 2 in rheumatoid arthritis synovial fibroblasts. Arthritis Rheum. 2009;60(2):355-63.
8. Hisamatsu T, Suzuki M, Podolsky DK. Interferon-gamma augments CARD4/NOD1 gene and protein expression through interferon regulatory factor-1 in intestinal epithelial cells. J Biol Chem. 2003;278(35):32962-8.
9. Fritz JH, Girardin SE, Fitting C, Werts C, Mengin-Lecreulx D, Caroff M, et al. Synergistic stimulation of human monocytes and dendritic cells by Toll-like receptor 4 and NOD1- and NOD2-activating agonists. Eur J Immunol. 2005;35(8):2459-70.
10. Chamaillard M, Hashimoto M, Horie Y, Masumoto J, Qiu S, Saab L, et al. An essential role for NOD1 in host recognition of bacterial peptidoglycan containing diaminopimelic acid. Nat Immunol. 2003;4(7):702-7.
11. Viala J, Chaput C, Boneca IG, Cardona A, Girardin SE, Moran AP, et al. Nod1 responds to peptidoglycan delivered by the Helicobacter pylori cag pathogenicity island. Nat Immunol. 2004;5(11):1166-74.
12. Welter-Stahl L, Ojcius DM, Viala J, Girardin S, Liu W, Delarbre C, et al. Stimulation of the cytosolic receptor for peptidoglycan, Nod1, by infection with Chlamydia trachomatis or Chlamydia muridarum. Cell Microbiol. 2006;8(6):1047-57.
13. Opitz B, Puschel A, Beermann W, Hocke AC, Forster S, Schmeck B, et al. Listeria monocytogenes activated p38 MAPK and induced IL-8 secretion in a nucleotide-binding oligomerization domain 1-dependent manner in endothelial cells. J Immunol. 2006;176(1):484-90.
14. van Heel DA, Ghosh S, Butler M, Hunt K, Foxwell BM, Mengin-Lecreulx D, et al. Synergistic enhancement of Toll-like receptor responses by NOD1 activation. Eur J Immunol. 2005;35(8):2471-6.
15. McGovern DP, Hysi P, Ahmad T, van Heel DA, Moffatt MF, Carey A, et al. Association between a complex insertion/deletion polymorphism in NOD1 (CARD4) and susceptibility to inflammatory bowel disease. Hum Mol Genet. 2005;14(10):1245-50.
16. Hysi P, Kabesch M, Moffatt MF, Schedel M, Carr D, Zhang Y, et al. NOD1 variation, immunoglobulin E and asthma. Hum Mol Genet. 2005;14(7):935-41.

17. Arnett FC, Edworthy SM, Bloch DA, McShane DJ, Fries JF, Cooper NS, et al. The American Rheumatism Association 1987 revised criteria for the classification of rheumatoid arthritis. Arthritis Rheum. 1988;31(3):315-24.
18. Ospelt C, Brentano F, Jungel A, Rengel Y, Kolling C, Michel BA, et al. Expression, Regulation, and Signaling of the Pattern-Recognition Receptor Nucleotide-Binding Oligomerization Domain 2 in Rheumatoid Arthritis Synovial Fibroblasts. Arthritis and Rheumatism. 2009;60(2):355-63.
19. Joosten LA, Heinhuis B, Abdollahi-Roodsaz S, Ferwerda G, Lebourhis L, Philpott DJ, et al. Differential function of the NACHT-LRR (NLR) members Nod1 and Nod2 in arthritis. Proc Natl Acad Sci U S A. 2008;105(26):9017-22.
20. Yoo NJ, Park WS, Kim SY, Reed JC, Son SG, Lee JY, et al. Nod1, a CARD protein, enhances pro-interleukin-1beta processing through the interaction with pro-caspase-1. Biochem Biophys Res Commun. 2002;299(4):652-8.
21. van der Heijden IM, Wilbrink B, Tchetverikov I, Schrijver IA, Schouls LM, Hazenberg MP, et al. Presence of bacterial DNA and bacterial peptidoglycans in joints of patients with rheumatoid arthritis and other arthritides. Arthritis Rheum. 2000;43(3):593-8.
22. Williams KL, Lich JD, Duncan JA, Reed W, Rallabhandi P, Moore C, et al. The CATERPILLER protein monarch-1 is an antagonist of toll-like receptor-, tumor necrosis factor alpha-, and Mycobacterium tuberculosis-induced pro-inflammatory signals. J Biol Chem. 2005;280(48):39914-24.
23. Ting JP, Duncan JA, Lei Y. How the noninflammasome NLRs function in the innate immune system. Science. 2010;327(5963):286-90.

FIGURE LEGENDS

Figure 1. A) Representative pictures of NOD1 expression in RA and OA synovial tissues are shown. As negative controls, NOD1-blocking peptide (inset in upper panel) or isotype controls (inset in lower panel) were used. Nuclei were counterstained with hematoxylin. Positive staining appears in red. Stronger staining intensity of lining and sublining areas in RA patients was found after scoring (Mann-Whitney test. * = $p < 0.05$). B) RA synvovial tissues were double stained for NOD1 (green) and CD68 (red) for macrophages. C) RA synvovial tissues were double stained for NOD1 (green) and vimentin (red) for mesenchymal cells. Nuclei appear in blue (DAPI). Arrows point at double stained cells which are magnified in the insets. D) Strong staining for NOD1 was seen in synovial tissues from patients with gout, but not in patients with psoriasis arthritis (PA).

Figure 2. Expression of NOD1 mRNA and protein in RASFs, OASFs, healthy controls (HC) PBMCs and MDMs. A) Similar expression levels of NOD1 mRNA (n=4-5) and of NOD1 protein (n=5-6) were found in the various cell types tested. Delta Ct = cycle of threshold NOD1-cycle of threshold 18S; MFI = mean fluorescence intensity. **B)** After stimulation of RASFs (n=6) with Tri-DAP, Pam3, PIC, LPS, IL-1β or TNF-α for 24h, levels of NOD1 mRNA only significantly changed after PIC stimulation as calculated by Wilcoxon matched pairs test. Also, NOD1 protein was more abundant after 24h stimulation of RASFs with PIC (n=6; non-parametric Friedman test followed by Dunn's multiple comparison test). *=$p < 0.05$. **C)** NOD1 mRNA or protein expression did not change in MDMs (n=3) after incubation with TLR ligands for 24h.

Figure 3. Tri-DAP induces the production of proinflammatory cytokines, chemokines, matrix degrading enzymes and peptidoglycan-sensing PRRs in RASFs. Incubation of RASFs (n=6) with 10 ng/ml Tri-DAP for 8h and 24h significantly induced mRNA levels of

A) IL-6 and CCL5, and **B)** MMP-1, MMP-3, and MMP-13 but not MMP-9. From the measured pattern-recognition receptors only TLR2 (n=8) **(C)** and NOD2 (n=3-8) were significantly changed **(D).** Non-parametric Friedman test followed by Dunn's multiple comparison test was used. * = $p < 0.05$; ** = $p < 0.01$; *** = $p < 0.001$.

Figure 4. Tri-DAP specificity and NOD1 silencing. A) RASFs (n=2-6) were stimulated with Tri-DAP alone or Tri-DAP with polymyxin B for 24h and IL-6 levels in the cell supernatants were measured by ELISA. **B)** RASFs (n=3-4) were transfected with control siRNA (sc) or NOD1 targeting siRNA (siNOD1) and NOD1 mRNA and protein expression was measured 24h and 48h after transfection. **C)** 24h after transfection of RASFs (n=6) with NOD1 siRNA or scrambled control siRNA (sc), cell were stimulated for 24h with Tri-DAP and IL-6 was measured in the supernatants. Non-parametric Friedman test followed by Dunn's multiple comparison test was used. * = $p < 0.05$.

Figure 5. Silencing of NOD1 downregulates TLR2 and IL-1β induced IL-6 production. A) TwoWay ANOVA analysis showed synergistic interaction of Tri-DAP stimulation with Pam3 and LPS in the production of IL-6 in RASFs (n=6). **B)** Knock-down of NOD1 in RASFs (n=6) led to decreased levels of IL-6 after Pam3 stimulation when compared to control transfected RASFs by Wilcoxon matched pairs test (left panel). Knock-down of NOD2 did not induce any change in IL-6 levels after stimulation with Pam3 (n=4) (right panel). **C)** Stimulation with heat inactivated *Staphylococcus aureus* (SA) or *Listeria monocytogenes* (LM) resulted in similar levels of IL-6 in NOD1 siRNA and control transfected cells (n=6) (left panel). Also, mRNA levels of TLR2 did not differ between NOD1 silenced and control RASFs, but were induced by stimulation with Pam3 (n=3) (right panel). **(D)** IL-6 levels were significantly lower in siNOD1 transfected cells than in control transfected cells after stimulation with IL-1β (n=6). Wilcoxon matched pairs test was used for

calculations. * = $p < 0.05$; ** = $p < 0.01$.

Figure 6. NOD1 influences IRAK1 phosphorylation. IRAK1 phosphorylation significantly increased after stimulation of control transfected RASFs with Pam3 for 20min, but not in NOD1 siRNA transfected cells (n=15). Wilcoxon matched pairs test was used for calculations. ** = $p < 0.01$

Supplemental Figure 1. Increased production of CCL5, MMPs, TLR2 and NOD2 protein after Tri-DAP stimulation. RASFs were incubated with 10 ng/ml Tri-DAP and levels of **A)** CCL5 (n=8) and **B)** MMP-1 (n=8) and MMP-3 (n=6) were measured in the supernatants by ELISA after 24h. Wilcoxon matched pairs test was used for calculations. * = $p < 0.05$; ** = $p < 0.01$. **C)** TLR2 protein was measured in RASFs 24h after stimulation with 10 ng/ml Tri-DAP by flow cytometry. **D)** NOD2 protein levels were determined by Western blotting 48h after stimulation with 10 ng/ml Tri-DAP or 10 ng/ml TNF-α (n=2).

Supplemental Figure 2. Time course of the induction of IL-6, CCL5, MMPs, TLR2 and NOD2 after Tri-DAP stimulation. RASFs (n=3) were incubated with 10 μg/ml Tri-DAP for the indicated time points and transcripts of **A)** IL-6, **B)** CCL5, **C)** MMP-1, MMP-3, MMP-9, MMP-13, and **D)** TLR2 and NOD2 were determined by real-time PCR. One representative time course experiment out of 3 is shown.

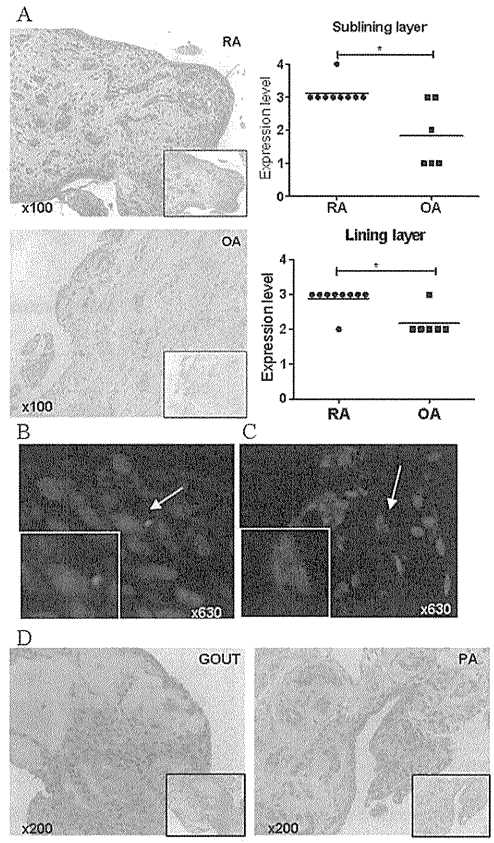

Figure 1. A) Representative pictures of NOD1 expression in RA and OA synovial tissues are shown. As negative controls, NOD1-blocking peptide (inset in upper panel) or isotype controls (inset in lower panel) were used. Nuclei were counterstained with hematoxylin. Positive staining appears in red. Stronger staining intensity of lining and sublining areas in RA patients was found after scoring (Mann-Whitney test. * = $p < 0.05$). **B)** RA synvovial tissues were double stained for NOD1 (green) and CD68 (red) for macrophages. **C)** RA synvovial tissues were double stained for NOD1 (green) and vimentin (red) for mesenchymal cells. Nuclei appear in blue (DAPI). Arrows point at double stained cells which are magnified in the insets. **D)** Strong staining for NOD1 was seen in synovial tissues from patients with gout, but not in patients with psoriasis arthritis (PA).

200x480mm (300 x 300 DPI)

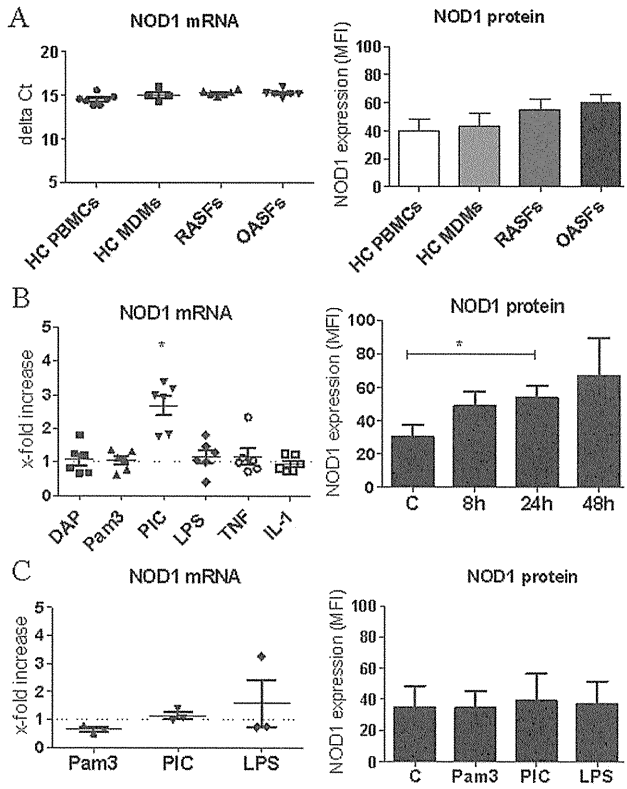

Figure 2. Expression of NOD1 mRNA and protein in RASFs, OASFs, healthy controls (HC) PBMCs and MDMs. A) Similar expression levels of NOD1 mRNA (n=4-5) and of NOD1 protein (n=5-6) were found in the various cell types tested. Delta Ct = cycle of threshold NOD1-cycle of threshold 18S; MFI = mean fluorescence intensity. B) After stimulation of RASFs (n=6) with Tri-DAP, Pam3, PIC, LPS, IL-1b or TNF-a for 24h, levels of NOD1 mRNA only significantly changed after PIC stimulation as calculated by Wilcoxon matched pairs test. Also, NOD1 protein was more abundant after 24h stimulation of RASFs with PIC (n=6; non-parametric Friedman test followed by Dunn's multiple comparison test). *=$p < 0.05$. C) NOD1 mRNA or protein expression did not change in MDMs (n=3) after incubation with TLR ligands for 24h.

83x158mm (300 x 300 DPI)

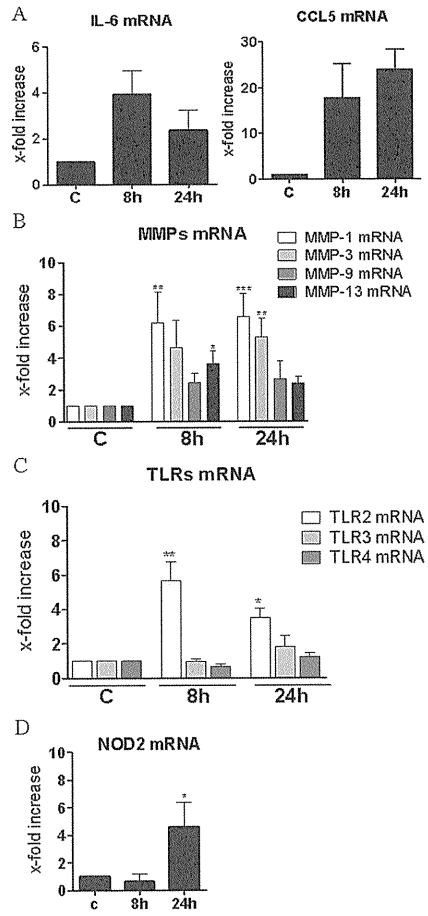

Figure 3. Tri-DAP induces the production of proinflammatory cytokines, chemokines, matrix degrading enzymes and peptidoglycan-sensing PRRs in RASFs. Incubation of RASFs (n=6) with 10 ng/ml Tri-DAP for 8h and 24h significantly induced mRNA levels of A) IL-6 and CCL5, and B) MMP-1, MMP-3, and MMP-13 but not MMP-9. From the measured pattern-recognition receptors only TLR2 (n=8) (C) and NOD2 (n=3-8) were significantly changed (D). Non-parametric Friedman test followed by Dunn's multiple comparison test was used. * = $p < 0.05$; ** = $p < 0.01$; *** = $p < 0.001$.

76x214mm (300 x 300 DPI)